

Analysis and Predictability for Tipping Points with Leading-Order Nonlinear Terms

Francesco Romano* and Christian Kuehn†

May 3, 2018

Abstract

Tipping points have been actively studied in various applications as well as from a mathematical viewpoint. A main technique to theoretically understand early-warning signs for tipping points is to use the framework of fast-slow stochastic differential equations. A key assumption in many arguments for the existence of variance and auto-correlation growth before a tipping point is to use a linearization argument, i.e., the leading-order term governing the deterministic (or drift) part of stochastic differential equation is linear. This assumption guarantees a local approximation via an Ornstein-Uhlenbeck process in the normally hyperbolic regime before, but sufficiently bounded away from, a bifurcation. In this paper, we generalize the situation to leading-order nonlinear terms for the setting of one fast variable. We work in the quasi-steady regime and prove that the fast variable has a well-defined stationary distribution and we calculate the scaling law for the variance as a bifurcation-induced tipping point is approached. We cross-validate the scaling law numerically. Furthermore, we provide a computational study for the predictability using early-warning signs for leading-order nonlinear terms based upon receiver-operator characteristic curves.

Keywords: critical transition, tipping point, warning sign, scaling law, bifurcation, fast-slow system, stochastic differential equation, ROC curve, predictability.

1 Introduction

Tipping points (or critical transitions) have been studied intensively in recent years with a focus on finding early-warning signs [1, 11, 15]. One key idea to predict a transition is to exploit the effect of critical slowing down indirectly via observing a noisy time series of a dynamical system. The idea goes back (at least) to the work of Wiesenfeld [16] but has gained recent popularity

*Faculty of Mathematics, Technical University of Munich, Boltzmannstr. 3, 85747 Garching b. Munich, Germany & Ludwig-Maximilians-Universitaet, Elite Graduate Course Theoretical and Mathematical Physics, Theresienstr. 37, 80333, Munich, Germany.

†Faculty of Mathematics, Technical University of Munich, Boltzmannstr. 3, 85747 Garching b. Munich, Germany

in many contexts, particularly in ecology [4] and climate science [5]. In terms of a fast-slow stochastic differential equation, the simplest class of examples are systems of the form

$$\begin{aligned} du &= f(u, v) dt + \sigma dW, \\ dv &= \varepsilon dt, \end{aligned} \tag{1}$$

where $u = u(t), v = v(t) \in \mathbb{R}$, W is a one-dimensional Brownian motion, $\sigma > 0$ controls the noise level, and $\varepsilon > 0$ is a small parameter. Note that u is a fast variable in comparison to the slow variable v as ε is small. If one wants to model the simplest situations, when a bifurcation-induced tipping occurs, one usually selects for the drift term $f(u, v)$ a normal form [7, 13] for a bifurcation such as $f(u, v) = v - u^2$ for the fold or $f(u, v) = uv - u^3$ for the (sub-critical) pitchfork [2]. Even many higher-dimensional cases have been analyzed by now [11] for fast-slow SODEs. Let us suppose that the drift term has a non-hyperbolic steady state at $(u, v) = (0, 0)$, or alternatively formulated the normal hyperbolicity of the critical manifold

$$\mathcal{C}_0 = \{(u, v) \in \mathbb{R}^2 : f(u, v) = 0\}$$

breaks down at the origin. Furthermore, assume that the critical manifold has one component, which is attracting for the fast dynamics and locally parametrized by $\mathcal{C}_0^a = \{u = h(v)\} \subset \mathcal{C}_0$ for some smooth function h and $(0, 0)$ lies on the boundary of \mathcal{C}_0^a . The standard tool to understand the local fluctuations of the stochastic process u near the origin is now to consider the linearized non-autonomous system along \mathcal{C}_0^a

$$dU = D_u f(h(\varepsilon t), \varepsilon t) U dt + \sigma dW =: A(\varepsilon t) U dt + \sigma dW. \tag{2}$$

Of course, (2) is just a standard one-dimensional non-autonomous Ornstein-Uhlenbeck (OU) process. In the quasi-steady (or adiabatic) limit $\varepsilon \rightarrow 0$, the process becomes autonomous and can be viewed as a parametrized family since the variable v is fixed and can then be viewed as a parameter v ; to emphasize when this viewpoint is taken we shall write $p = v$. The solution of the resulting OU process is easy to calculate [6]. If we let $V_\infty = \lim_{t \rightarrow \infty} \text{Var}(U(t))$ be the time-asymptotic variance then one finds for the fold and pitchfork examples above

$$V_{\infty, \text{fold}} = \mathcal{O}(p^{-1/2}), \quad V_{\infty, \text{pitchfork}} = \mathcal{O}(p^{-1}) \quad \text{as } p \nearrow 0, \tag{3}$$

i.e., the linearized leading-order approximation of the variance of the process u diverges with certain universal exponents as p tends to the bifurcation point. Note that the linear approximation only holds for sufficiently small noise and breaks down for the system with $0 < \varepsilon \ll 1$ in a very small ε -dependent neighbourhood of the origin [11] but it provides a very good approximation otherwise. Hence, variance growth can often be used as an early-warning sign for bifurcation-induced tipping. However, we did make the key assumption that linear terms are of leading-order. In this paper, we study leading-order nonlinear terms, which preclude the use of results from linear stochastic processes.

In Section 2 we provide the mathematical background and framework for our setting. In Section 3, we prove a variance scaling law for polynomial nonlinearities pU^k (k odd) and cross-validate it numerically. The universal scaling exponent can be computed explicitly and divergence of the variance is given by

$$V_{\infty, \text{nonlin}} = \mathcal{O}(p^{-2/(k+1)}) \quad \text{as } p \nearrow 0.$$

In Section 4, we provide a computational study to better understand practical predictability for leading-order nonlinear terms using receiver-operator characteristic (ROC) curves [12, 3, 17] in comparison to the linear case and also depending upon sliding window length, lead time, and alarm volume size.

2 Background and Framework

Consider the following ordinary differential equation (ODE) depending on the parameter $p \in \mathbb{R}$

$$\frac{dU}{dt} = pU^k, \quad U = U(t) \in \mathbb{R}, \quad U_0 := U(0), \quad (4)$$

and assume $k \in \mathbb{N}$ to be odd. The point $U_* = 0$ is a steady state for (4). One easily checks using the gradient structure of one-dimensional ODEs that U_* is (even globally) stable for $p < 0$ and unstable for $p > 0$. In particular, (4) has a bifurcation, respectively a bifurcation-induced tipping, when $p = 0$. Since we are interested in early-warning signs in the SODE case, we now study

$$dU = pU^k dt + \sigma dW, \quad U(0) = U_0, \quad (5)$$

where $\sigma > 0$, W a one-dimensional Brownian motion on a filtered probability space $(\mathbb{R}, \mathcal{F}, \mathcal{F}_t, \mathbb{P})$ and U_0 is a \mathcal{F}_0 -measurable random variable. In the following, we are going to show that the variance of the (unique global) solution $U(t)$ to (5) has a divergent behavior as $p \nearrow 0$. We are going to exploit the Fokker-Planck equation to find an explicit expression for the asymptotic variance

$$V_\infty := \lim_{t \rightarrow \infty} \text{Var}(U(t))$$

in Theorem 3.1. First, we provide some background. The SODE (5) has a unique global-in-time solution up to equivalence for any odd k .

Theorem 2.1. *For $p < 0$ and any $t > 0$, the stochastic process*

$$U(t) = U_0 + p \int_0^t U^k(s) ds + \sigma W(t)$$

is the unique solution (up to equivalence) to (5).

Proof. According to [10, Thm. 3.5], it is enough to prove that there exists a non-negative $C^{1,2}$ function ψ on $[0, \infty) \times \mathbb{R}^m$ such that for some constant $c > 0$

$$L\psi \leq c\psi \quad \text{and} \quad \psi_R = \inf_{|x| > R} \psi(t, x) \rightarrow \infty \text{ as } R \rightarrow \infty,$$

where

$$L\psi(s, x) = \partial_s \psi(s, x) + pX_s^k \partial_x \psi(s, x) + \frac{\sigma^2}{2} \partial_{xx} \psi(s, x).$$

We set $\psi(s, x) = (x^2 + 1)^a$ for $a > 1$. ψ is obviously $C^{1,2}$ and it satisfies

$$\psi_R = \inf_{|x| > R} \psi(t, x) = \inf_{|x| > R} (x^2 + 1)^a = (R^2 + 1)^a \rightarrow \infty \text{ as } R \rightarrow \infty.$$

It is only left to prove that for some $c > 0$ it holds $L\psi \leq c\psi$. We compute $L\psi$ to obtain:

$$\begin{aligned}
L\psi(s, x) &= \partial_s(x^2 + 1)^a + px^k \partial_x(x^2 + 1)^a + \frac{\sigma^2}{2} \partial_{xx}(x^2 + 1)^a \\
&= 2pax^{k+1}(x^2 + 1)^{a-1} + a\sigma^2(x^2 + 1)^{a-1} + 2a(a-1)\sigma^2 x^2(x^2 + 1)^{a-2} \\
&\leq a\sigma^2(x^2 + 1)^{a-1} + 2a(a-1)\sigma^2 x^2(x^2 + 1)^{a-2} \\
&\leq a\sigma^2(x^2 + 1)^{a-1} + 2a(a-1)\sigma^2(x^2 + 1)^{a-1} \\
&= [a\sigma^2 + 2a(a-1)\sigma^2](x^2 + 1)^{a-1} \\
&\leq [a\sigma^2 + 2a(a-1)\sigma^2](x^2 + 1)^a = [a\sigma^2 + 2a(a-1)\sigma^2]\psi(s, x),
\end{aligned}$$

where we used $p < 0, a > 0$ and the fact that $k + 1$ is even. Hence, the claim follows. \square

We recall that, under certain conditions, solutions to SODEs are Markov processes and under stronger assumptions their distribution converge in time to a stationary distribution, which can be identified with the solution to Fokker-Planck equation. Specifically, the following holds (see [10, Sec. 4.4-4.7, Lem. 4.16]):

Theorem 2.2. *Consider a stochastic differential equation of the form*

$$dU = g(U) dt + \sigma dW, \quad U = U(t) \in \mathbb{R}. \quad (6)$$

Suppose there exists a bounded open domain $\Omega \subset \mathbb{R}$ with regular boundary Γ such that

1. *If $x \in \mathbb{R} \setminus \Omega$, the mean time τ at which a path starting from x reaches the set Ω is finite,*
2. *$\sup_{x \in K} \mathbb{E}^x[\tau] < \infty$ for every compact set $K \subset \mathbb{R}$.*

Then, the Markov process $U = U(t)$ has a unique stationary distribution μ and, independently of the distribution of U_0 , the distribution of U converges to μ as $t \rightarrow +\infty$. Moreover, $\mu(A)$ has stationary density $\rho^{\text{st}}(x)$ with respect to Lebesgue measure, given by the unique (normalized) bounded solution of the stationary Fokker-Planck equation

$$L^* \rho^{\text{st}} := \frac{\sigma^2}{2} \partial_{xx} \rho^{\text{st}}(x) - \partial_x(f(x) \rho^{\text{st}}(x)) = 0. \quad (7)$$

If we can apply Theorem 2.2, and if we can compute the stationary solution ρ^{st} and from it the variance, then we can circumvent any OU processes used for the linear case.

3 Asymptotic Result for the Variance

We now show that Theorem 2.2 can be used to derive an asymptotic result for the variance of (5):

Theorem 3.1 (variance scaling law). *Suppose $p < 0$ and consider the one-dimensional non-linear SDE*

$$dU = pU^k dt + \sigma dW, \quad U(0) = U_0 \quad (8)$$

where U_0 is an \mathcal{F}_0 -measurable random variable. For each odd $k \in \mathbb{N}$, the associated deterministic ODE has a bifurcation in $p = 0$. Consider the stationary distribution ρ^{st} of the solution U_t to (8) and denote its variance by V_∞ . The following holds for all odd $k \in \mathbb{N}$:

$$V_\infty = \left(-\frac{k+1}{2p} \right)^{2/(k+1)} \frac{\Gamma(1+3/(k+1))}{\Gamma(1+1/(k+1))}, \quad (9)$$

where Γ is the usual Gamma function. In particular, for all odd k , the asymptotic behavior as $p \nearrow 0$ is given by

$$V_\infty = \mathcal{O}\left(\frac{1}{p^{2/(k+1)}}\right). \quad (10)$$

Proof. The proof proceed as follows: first, we show that our system satisfies the conditions in Theorem 2.2, so that we can use Fokker-Planck equation to compute the stationary distribution; then, we compute explicitly the solution to the Fokker-Planck equation and its variance to conclude the proof.

Step 1: Convergence to the asymptotic distribution. Fix $\Omega = (-R, R)$, which is open and bounded. To check the first condition in Theorem 2.2, it is enough to prove by Theorem 2.1 and [10, Thm. 3.9] that there exists in $[0, +\infty) \times (\mathbb{R} \setminus \Omega)$ a nonnegative function $\Psi(s, x) \in C^{1,2}$ such that

$$L\Psi(s, x) \leq -\alpha(s),$$

where $\alpha(s) \geq 0$ is a function such that

$$\beta(t) = \int_0^t \alpha(s) \, ds \rightarrow \infty \text{ as } t \rightarrow \infty.$$

We choose $\Psi(s, x) = (1 + x^2)^a$, $a > 1$, which satisfies the regularity hypothesis. Moreover,

$$\begin{aligned} L\Psi(s, x) &= 2pax^{k+1}(x^2 + 1)^{a-1} + a\sigma^2(x^2 + 1)^{a-1} + 2a(a-1)\sigma^2x^2(x^2 + 1)^{a-2} \\ &\leq [pax^{k+1} + a\sigma^2 + 2a(a-1)\sigma^2](x^2 + 1)^{a-1}. \end{aligned}$$

Choosing R big enough we can guarantee

$$pax^{k+1} + a\sigma^2 + 2a(a-1)\sigma^2 < -v$$

for all $x \in (\mathbb{R} \setminus \Omega) =: \Omega^c$ and some constant $v > 0$. This implies

$$L\Psi(s, x) \leq v(R^2 + 1)^{a-1} =: \alpha.$$

Furthermore, we have

$$\beta(t) = \int_0^t \alpha \, ds = \alpha t \rightarrow \infty \text{ as } t \rightarrow \infty$$

as required. This proves the first condition in Theorem 2.2. For the second condition, by [10, Thm. 3.9], the expectation of the random variable $\beta(\tau_{\Omega^c})$ exists and satisfies the inequality

$$\mathbb{E}^{s,x}[\beta(\tau_{\Omega^c})] \leq \beta(s) + \Psi(s, x),$$

which implies

$$\mathbb{E}^{s,x}[\tau_{\Omega^c}] \leq s + \frac{(1 + x^2)^a}{\alpha}.$$

Now, setting $s = 0$ we have

$$\mathbb{E}^x[\tau_{\Omega^c}] \leq \frac{(1+x^2)^a}{\alpha} < \infty \text{ for all compact sets } K.$$

Therefore, Theorem 2.2 implies that the density of $U(t)$ converges to ρ^{st} as $t \rightarrow +\infty$, independently of the initial condition U_0 .

Step 2: Density computation. ρ^{st} is the unique bounded (normalized) solution to the stationary Fokker-Planck equation

$$0 = -\partial_x [px^k \rho^{\text{st}}(x)] + \frac{1}{2} \partial_{xx} \rho^{\text{st}}(x). \quad (11)$$

In our case, one can simply compute by direct integration that

$$2py^k \rho^{\text{st}}(y) = \partial_y \rho^{\text{st}}(y) - \partial_y \rho^{\text{st}}(0)$$

Assume $\partial_x \rho^{\text{st}}(0) = 0$. Since we are looking for the unique bounded solution of (11), we can justify our assumption a posteriori by showing that the solution we obtain is bounded. We solve the last equation and obtain

$$\rho^{\text{st}}(x) = \rho^{\text{st}}(0) \exp\left(\frac{2p}{k+1} x^{k+1}\right).$$

Since $p < 0$ and $k+1$ is even, the exponential in the above expression can be integrated over \mathbb{R} . The constant $\rho^{\text{st}}(0)$ is the normalizing constant so we get

$$\rho^{\text{st}}(x) = \frac{\exp\left(\frac{p}{m} x^{2m}\right)}{\int_{\mathbb{R}} \exp\left(\frac{p}{m} x^{2m}\right) dx},$$

where $k+1 = 2m$ and $m \in \mathbb{N}$. This shows in particular that ρ^{st} is bounded, as required.

Step 3: Asymptotic variance. Since ρ^{st} is symmetric, its expected value is 0. Its variance is then given by

$$\begin{aligned} V_{\infty} &= \frac{1}{\int_{\mathbb{R}} \exp\left(\frac{p}{m} x^m\right) dx} \int_{\mathbb{R}} x^2 \exp\left(\frac{p}{m} x^{2m}\right) dx \\ &= \frac{2/3(-p/m)^{-3/2m} \Gamma(1 + 3/2m)}{2/3(-p/m)^{-1/2m} \Gamma(1 + 1/2m)} \\ &= \left(-\frac{1}{p}\right)^{1/m} \frac{\Gamma(1 + 3/2m) m^{1/m}}{\Gamma(1 + 1/2m)}. \end{aligned}$$

This concludes the proof. □

We remark that the approach we followed is quite general and it has not much to do with specific properties of (8) except it being a scalar equation. For higher-dimensional cases, we would have to use approximation and/or reduction methods to understand stationary solutions of the Fokker-Planck equation [14].

To cross-validate the theoretical result, we plot in Figure 1 a numerical approximation of the asymptotic variance for $k = 3$ obtained in the following way:

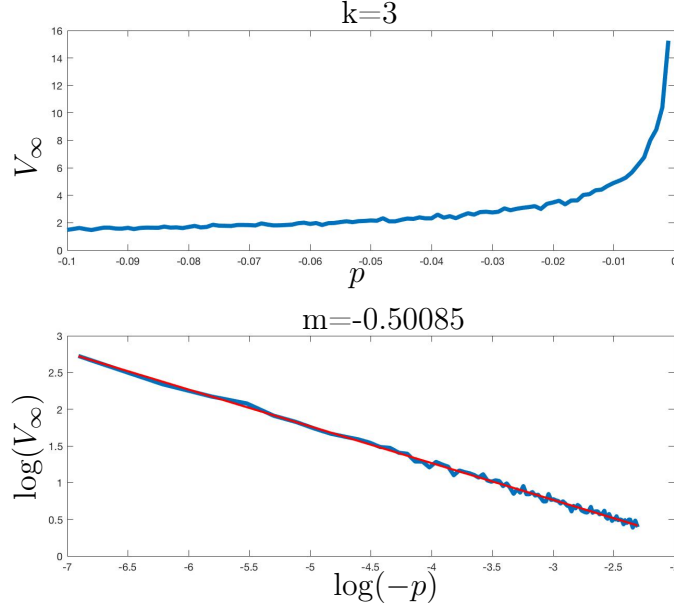


Figure 1: For $p \in [-0.1, 0]$ we solve the equation $du = pu^3 dt + dW_t$ on the interval $[0, 100]$ with initial condition $u_0 = 1$ using the Euler-Maruyama approximation method with $N = 1000$ time steps. The plot above shows the numerically approximated variance V_∞ from 1000 sample paths and $t^* = 100$. The loglog plot below (blue) shows clearly the (inverse) polynomial dependence. In red we plot the linear interpolation.

- (N1) first, we consider a sequence p_i converging to the bifurcation in $p = 0$ as $i \rightarrow \infty$;
- (N2) then, we choose (for each p_i) a large enough value $t = t^*$ so that the variance can be assumed to be close to the asymptotic limit;
- (N3) finally, using Euler-Maruyama method [9] we simulate a large enough number of sample paths to the SDE (5) so that the empirical variance can be accurately computed.

We remark here that the values of t^* and the number of sample paths have been chosen empirically via numerical simulations to ensure the required conditions to be satisfied. In Figure 1 we also show a loglog plot to highlight more clearly the relation of the form

$$V_\infty = \mathcal{O}\left(\frac{1}{p^m}\right).$$

The following table shows the results for odd values of k between 3 and 11:

k	m	$2/(k+1)$
3	-0.50085	-0.5
5	-0.33714	-0.3333
7	-0.24961	-0.25
9	-0.20656	-0.2
11	-0.17154	-0.1667

As one can see by comparing the second and third column, the numerical results are really close to the analytical analysis, so it is also possible to observe the scaling in direct practical simulations and/or data.

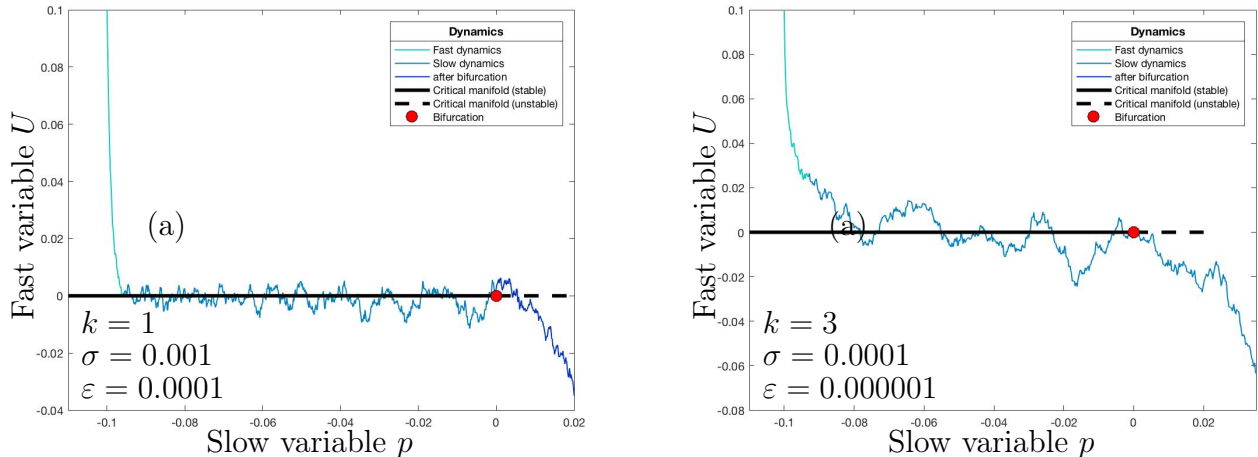


Figure 2: (a) $k = 1$, $(p_0, U_0) = (-0.1, 0.1)$, $\sigma = 0.001$, $\varepsilon = 0.0001$. (b) $k = 3$, $(p_0, U_0) = (-0.1, 0.1)$, $\sigma = 0.0001$, $\varepsilon = 0.000001$.

4 Statistics for early-warning signs

We continue to study (5) and want to determine, how well statistical classifiers based on our previous findings can be used to predict tipping points [3, 8, 12, 17]. Returning to our model class (1) we include in (5) the evolution of the parameter and study

$$\begin{cases} dU = \frac{p}{\varepsilon} U^k ds + \frac{\sigma}{\sqrt{\varepsilon}} dW, \\ dp = ds, \end{cases} \quad (12)$$

where $s = \varepsilon t$, and we can also view the system as a single non-autonomous SODE

$$dU(p) = \frac{p}{\varepsilon} U^k(p) dp + \frac{\sigma}{\sqrt{\varepsilon}} dW(p). \quad (13)$$

$\mathcal{C}_0^a := \{U = 0, p < 0\}$ contains attracting steady states: if the parameter is initially negative, the evolution converges to \mathcal{C}_0^a (fast dynamics) and then remains close to it (slow dynamics) until tipping happens. Simulations for different choices of the initial conditions (p_0, U_0) , the nonlinearity parameters k , and the parameters σ and ε are shown in Figure 2.

Having defined the test model, we specify the setting, in which our predictions happen and the object we want to predict. Consider $U(s)$ and assume we have a time series of w observations acquired at evenly spaced time intervals of length Δs , starting from time s_{n-w+1} to time s_n . At time s_n we want to predict, whether a bifurcation happens at a future time in the interval $[s_{n+\kappa-\delta}, s_{n+\kappa+\delta}]$. We call κ the lead time of our prediction, δ the uncertainty and w the sliding window width. Given a single time series (or “realization”) over the time window $[s_{n-w+1}, s_n]$, we approximate the variance via a sliding window estimate

$$v_n = \frac{1}{w} \sum_{i=n-w+1}^n (U(s_i) - \bar{U}(s_n))^2, \text{ where } \bar{U}(s_n) = \frac{1}{w} \sum_{i=n-w+1}^n U(s_i).$$

Qualitatively, the reason for using the sliding variance is that, if ε is small enough, we can assume the parameter p to be approximately constant in the sliding window.

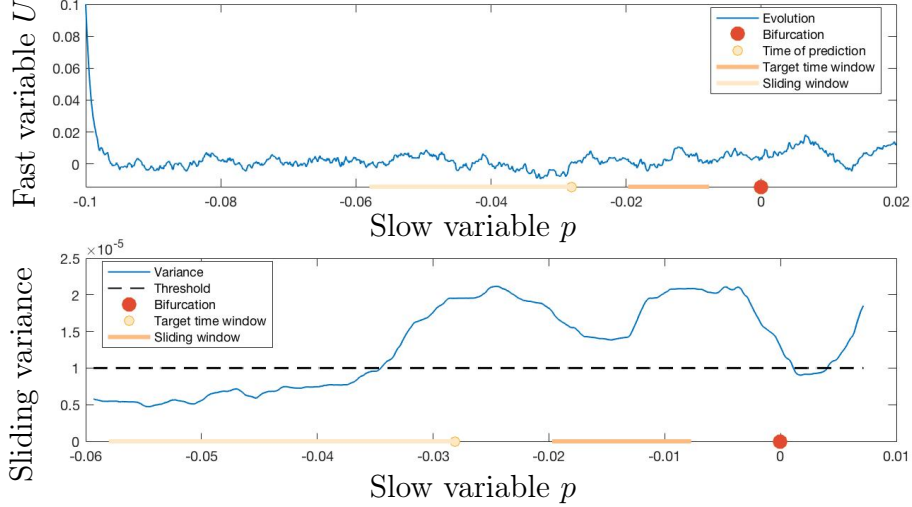


Figure 3: An example of false positive prediction: the bifurcation happens outside the target interval and therefore the correct value of our estimator is 0 (i.e. no bifurcation); the plot below shows the values of the sliding variance and the sliding variance is above the threshold so our estimator wrongly classifies this as a positive prediction.

Now we define a family of binary estimators as follows: we raise an alarm for a tipping when the value of the variance goes above the threshold d . We define the indicator function for the alarm volume as follows

$$A_n(v_n, d) = \begin{cases} 1 & \text{if } v_n \geq d, \\ 0 & \text{otherwise.} \end{cases} \quad (14)$$

To clarify the prediction procedure we show two examples in Figure 3 and Figure 4. In each example both the evolution of the fast-slow system and the sliding variance are shown. In particular, in the plot of the sliding variance we have highlighted the threshold level (black dashed line), the sliding window used to compute the variance (yellow), the interval $[s_{n+\kappa-\delta}, s_{n+\kappa+\delta}]$ (orange) and the bifurcation point (red). The time at which the prediction is performed is marked with a yellow dot.

Now one defines *true* and *false positive rates* as

$$TPR(M) = \frac{\#\{x: x \text{ is true positive}\}}{\#\{x: x \text{ is positive}\}} \quad \text{and} \quad FPR(M) = \frac{\#\{x: x \text{ is false positive}\}}{\#\{x: x \text{ is negative}\}}.$$

A standard way to represent the efficiency of the classifier is then to plot the graph FPR vs TPR. The space having FPR on the x -axis and TPR on the y -axis is called *ROC space*. In ROC space a good classifier is very close to the point $(0, 1)$, which represents the perfect classifier. Note also that the diagonal (i.e. the line $FPR = TPR$) in the ROC space represents random guesses. Therefore, an obvious minimal requirement for the efficiency of a classifier is being represented above this line. Since our estimator depends on the threshold d , it will be represented as a curve in the ROC space, known as ROC curve.

We observe that the estimator we defined is statistically relevant for different values of the nonlinearity. In Figure 5 ROC curves are plotted for $k = 1$, $k = 3$ and $k = 5$ and parameter values

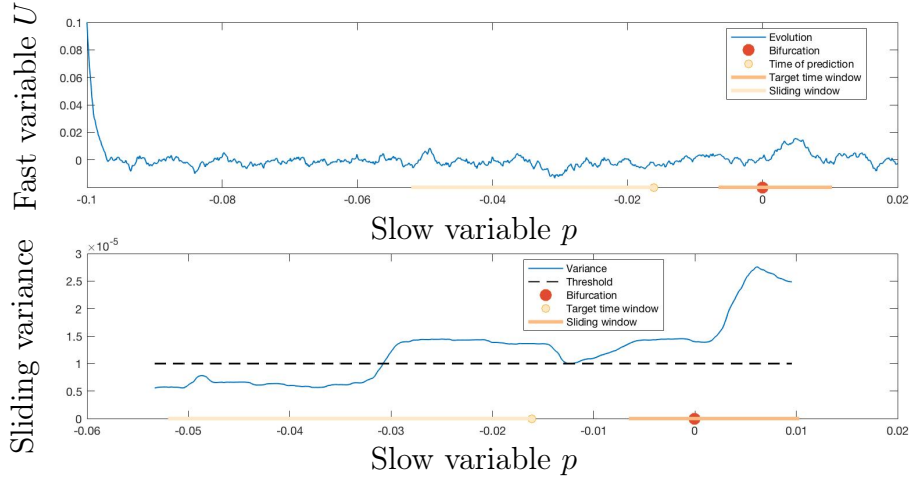


Figure 4: An example of true positive prediction: the bifurcation happens inside the target interval and therefore the correct value of our estimator is 1 (i.e. bifurcation); the plot below shows that the sliding variance is above the threshold. Hence, our estimator correctly classifies this as a positive prediction.

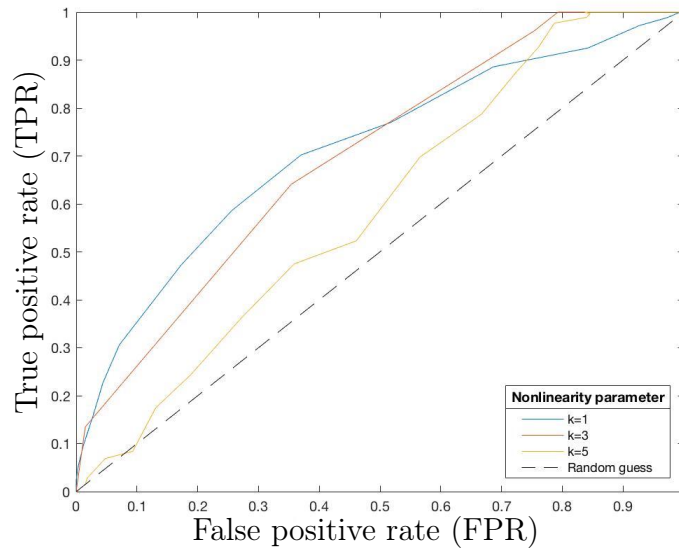


Figure 5: ROC curves for different values of the parameter k . Because the ROC curves are above the diagonal (the diagonal corresponds to random guesses), the estimator we propose is statistically relevant.

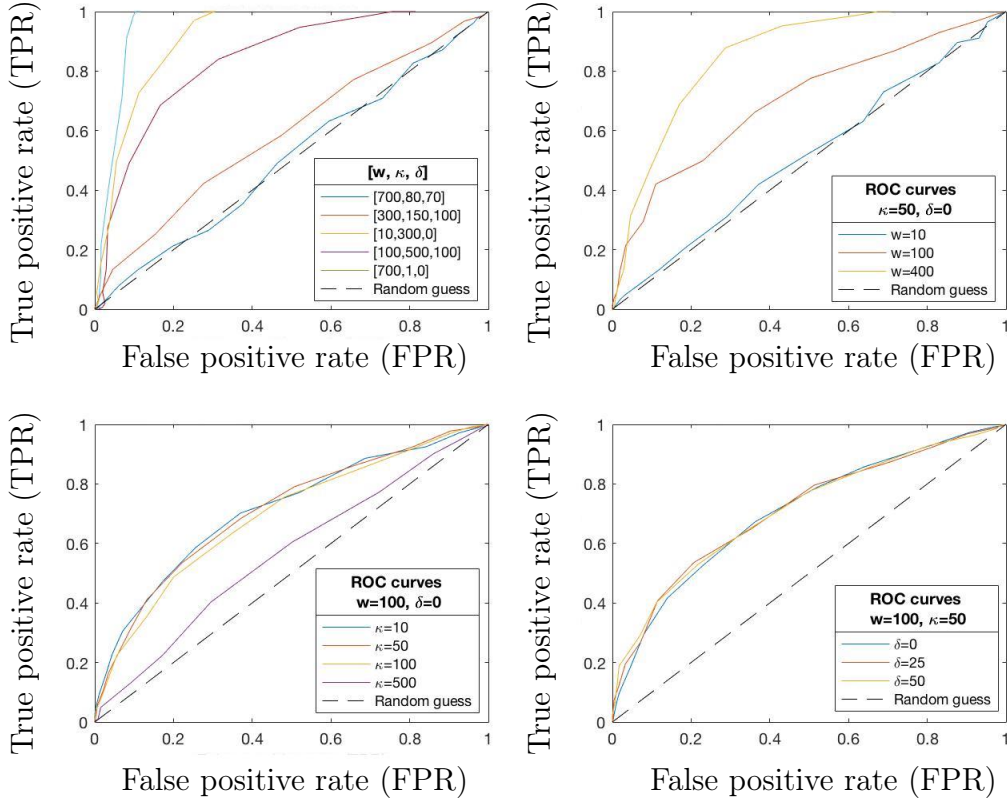


Figure 6: The four plots show different ROC curves in the nonlinear case $k = 3$. In the first plot ROC curves for different values of the parameters w, κ, δ are shown. The other plots show the comparison between different values of each parameter while the others remain fixed. These results have been obtained for $(U_0, p_0) = (0.1; -0.1)$, $\sigma = 10^{-5}$ and $\varepsilon = 10^{-8}$ averaging over 1000 sample paths obtained using Euler-Maruyama method with a grid of 10000 points.

- $[k, \kappa, \delta, w, \sigma, \varepsilon, N] = [1, 10, 0, 10^2, 10^{-3}, 10^{-4}, 10^3]$,
- $[k, \kappa, \delta, w, \sigma, \varepsilon, N] = [3, 10^3, 500, 3 \cdot 10^3, 10^{-5}, 10^{-8}, 10^5]$,
- $[k, \kappa, \delta, w, \sigma, \varepsilon, N] = [5, 10^3, 0, 3 \cdot 10^3, 5 \cdot 10^{-6}, 2.5 \cdot 10^{-9}, 10^4]$.

In the simulations we set the number of observations of a tipping even, i.e., the number of sample paths, to 1000. It is also interesting to fix a value of k and study the efficiency of our estimator as a function of the sliding window w , the lead time κ and the uncertainty δ . Intuitively, we expect the efficiency of the estimator to be positively correlated to w and δ , but negatively correlated to κ . This reflects the fact that a higher availability of data, as well as the possibility to allow bigger uncertainty, improves our predictive ability. On the other hand, if we try to predict the bifurcation far in advance (i.e. large lead time), we should obtain poorer results.

Figure 6 shows the case $k = 3$. Our expectations are confirmed by the data. A wider sliding window and a smaller lead time give better predictions. Surprisingly, the uncertainty δ seems to have no major impact on the results for the interval of values that we tested here. This hints at the conjecture that lead time and sliding window width are the major limiting factors for the parameter configurations we tested here.

Acknowledgements: CK would like to thank the VolkswagenStiftung for support via a Lichtenberg Professorship Grant.

References

- [1] P. Ashwin, S. Wieczorek, R. Vitolo, and P. Cox. Tipping points in open systems: bifurcation, noise-induced and rate-dependent examples in the climate system. *Phil. Trans. R. Soc. A*, 370:1166–1184, 2012.
- [2] N. Berglund and B. Gentz. *Noise-Induced Phenomena in Slow-Fast Dynamical Systems*. Springer, 2006.
- [3] C. Boettinger and A. Hastings. Quantifying limits to detection of early warning for critical transitions. *J. R. Soc. Interface*, 9(75):2527–2539, 2012.
- [4] S.R. Carpenter and W.A. Brock. Rising variance: a leading indicator of ecological transition. *Ecology Letters*, 9:311–318, 2006.
- [5] P.D. Ditlevsen and S.J. Johnsen. Tipping points: early warning and wishful thinking. *Geophys. Res. Lett.*, 37:19703, 2010.
- [6] C. Gardiner. *Stochastic Methods*. Springer, Berlin Heidelberg, Germany, 4th edition, 2009.
- [7] J. Guckenheimer and P. Holmes. *Nonlinear Oscillations, Dynamical Systems, and Bifurcations of Vector Fields*. Springer, New York, NY, 1983.
- [8] S. Hallerberg and H. Kantz. Influence of the event magnitude on the predictability of extreme events. *Phys. Rev. E*, 77:011108, 2008.
- [9] D.J. Higham. An algorithmic introduction to numerical simulation of stochastic differential equations. *SIAM Review*, 43(3):525–546, 2001.
- [10] R.Z. Khasminskii. *Stochastic Stability of Differential Equations*. Springer, 2011.
- [11] C. Kuehn. A mathematical framework for critical transitions: normal forms, variance and applications. *J. Nonlinear Sci.*, 23(3):457–510, 2013.
- [12] C. Kuehn, G. Zschaler, and T. Gross. Early warning signs for saddle-escape transitions in complex networks. *Scientific Reports*, 5:13190, 2015.
- [13] Yu.A. Kuznetsov. *Elements of Applied Bifurcation Theory*. Springer, New York, NY, 3rd edition, 2004.
- [14] H. Risken. *The Fokker-Planck Equation*. Springer, 1996.
- [15] M. Scheffer, J. Bascompte, W.A. Brock, V. Brovkhin, S.R. Carpenter, V. Dakos, H. Held, E.H. van Nes, M. Rietkerk, and G. Sugihara. Early-warning signals for critical transitions. *Nature*, 461:53–59, 2009.
- [16] K. Wiesenfeld. Noisy precursors of nonlinear instabilities. *J. Stat. Phys.*, 38(5):1071–1097, 1985.

- [17] X. Zhang, S. Hallerberg, and C. Kuehn. Predictability of critical transitions. *Phys. Rev. E*, 92:052905, 2015.